

# Metal-Rich A-Type Supergiants in M 31

By

Norbert Przybilla<sup>1</sup>, Keith Butler<sup>2</sup> & Rolf-Peter Kudritzki<sup>3</sup>

<sup>1</sup> Dr. Karl Remeis-Sternwarte Bamberg, Sternwartstrasse 7, D-96049 Bamberg, Germany

<sup>2</sup> Universitäts-Sternwarte München, Scheinerstrasse 1, D-81679 München, Germany

<sup>3</sup>Institute for Astronomy, 2680 Woodlawn Drive, Honolulu, HI 96822, USA

We discuss results of an exploratory non-LTE analysis of two metal-rich A-type supergiants in M 31. Using comprehensive model atoms we derive accurate atmospheric parameters from multiple indicators and show that non-LTE effects on the abundance determination can be substantial (by a factor 2-3). The non-LTE analysis removes systematic trends apparent in the LTE approach and reduces statistical uncertainties. Characteristic abundance patterns of the light elements provide empirical constraints on the evolution of metal-rich massive stars.

---

## 1. Introduction

Absorption by interstellar dust in the Galactic plane prohibits the study of the Milky Way in its entirety. A comprehensive global view of a giant spiral galaxy can be obtained only for the nearest neighbour of this class, the Andromeda galaxy (M 31). The old stellar population of this, the most luminous galaxy of the Local Group, turns out to be unexpectedly metal-rich (see e.g. van den Bergh 1999) and present-day abundances as traced by nebulae (H II regions, supernova remnants) also indicate a metal-rich character and the presence of abundance gradients in the disk (Dennefeld & Kunth 1981; Blair et al. 1982).

The current generation of large telescopes allows spectroscopy of luminous stars in M 31 to be carried out. Quantitative studies of massive blue supergiants (BSGs) can help to verify results from nebulae. In particular, analyses of bright BA-type supergiants (BA-SGs) facilitate abundance determinations to be extended beyond the light and  $\alpha$ -process elements to iron group and s-process species. This makes BA-SGs highly valuable for constraining the galactochemical evolution of M 31 empirically by tracing the abundance gradients. However, there is more to gain: observational constraints on the evolution of massive stars in a metal-rich environment, using BSGs as probes for mixing with nuclear-processed matter, and the potential to employ them as distance indicators via application of the flux-weighted gravity-luminosity relationship (FGLR, Kudritzki et al. 2003).

Only a few studies of individual BSGs in M 31 are available so far (Venn et al. 2000; Smartt et al. 2001; Trundle et al. 2002). These are based either on the assumption of LTE or on unblanketed non-LTE model atmospheres. Here, we present results of an exploratory study of two A-SGs in M 31. A hybrid non-LTE analysis technique is used which considers line blanketing and non-LTE line formation and is thus able to provide results of hitherto unachieved accuracy and consistency (Przybilla 2002; Przybilla et al. 2006).

## 2. Observations and model computations

Spectra of two luminous A-type supergiants in the north-eastern arm of M 31 were taken in November 2002 with ESI on the Keck II telescope. The Echelle spectra were reduced with the MAKEE package and our own IDL-based routines for order merging and continuum normalisation. Complete wavelength coverage of the spectra between  $\sim 3900$  and  $\sim 9300$  Å was obtained at high S/N ( $> 150$  in the visual) and moderately high resolution ( $R \simeq 8000$ ). The dataset is complemented by Keck I/HIRES spectra with a more limited wavelength coverage ( $R \simeq 35\,000$ , S/N  $\sim 80$ ) as utilised by Venn et al. (2000).

TABLE 1. Atmospheric and fundamental stellar parameters with uncertainties

Object	$T_{\text{eff}}$ (K)	$\log g$	He	[M/H]	$\xi/\zeta/v \sin i$ (km/s)	$\log L/L_{\odot}$	$M_e/M_{\odot}$	$M_s/M_{\odot}$	$R/R_{\odot}$
41-3654	9200	1.00	0.13	+0.13	8/20/36	5.63	29	24	257
(A2Iae)	150	0.05	0.02	0.06	1/ 5/ 5	0.04	4	4	15
41-3712	8550	1.00	0.13	-0.04	8/18/25	5.45	24	22	243
(A3Iae)	150	0.05	0.02	0.05	1/ 5/ 5	0.04	3	4	14

The model calculations are carried out in a hybrid non-LTE approach as discussed in detail by Przybilla et al. (2006). In brief, hydrostatic, plane-parallel and line-blanketed LTE model atmospheres are computed with ATLAS9 (Kurucz 1993; with further modifications: Przybilla et al. 2001). Then, non-LTE line formation is performed on the resulting model stratifications. The coupled radiative transfer and statistical equilibrium equations are solved and spectrum synthesis with refined line-broadening theories is performed using DETAIL and SURFACE. State-of-the-art non-LTE model atoms relying on data from *ab-initio* computations, avoiding rough approximations wherever possible, are utilised for the stellar parameter and abundance determination.

### 3. Stellar parameters and elemental abundances

The atmospheric parameters are derived spectroscopically from multiple indicators, following the methodology described by Przybilla et al. (2006). Effective temperature  $T_{\text{eff}}$  and surface gravity  $\log g$  are constrained from several non-LTE ionization equilibria (C I/II, N I/II, Mg I/II) and from modelling the Stark-broadened profiles of the higher Balmer and Paschen lines. The internal accuracy of the method allows the  $1\sigma$ -uncertainties to be reduced to  $\sim 1$ – $2\%$  in  $T_{\text{eff}}$  and to  $0.05$ – $0.10$  dex in  $\log g$ . Several He I lines are used to derive the helium abundance. The stellar metallicity relative to the solar standard [M/H] (logarithmic values) is determined from the heavier metals (O, Mg, S, Ti, Fe) in non-LTE. Microturbulent velocities  $\xi$  are obtained in the usual way by requiring abundances to be independent of line equivalent width – consistency is achieved from all non-LTE species. Finally, macroturbulences  $\zeta$  and rotational velocities  $v \sin i$  are determined from line profile fits. The results are summarised in Table 1, where information on the fundamental stellar parameters is also given: luminosity  $L$ , evolutionary and spectroscopic mass  $M_e/M_s$  and radius  $R$ . Photometric data of Massey et al. (2006) are adopted.

Elemental abundances are determined for several chemical species, with many of the astrophysically most interesting in non-LTE and the remainder in LTE, see Fig. 1. The two M31 supergiants are more metal-rich than the Galactic BA-SGs studied using the same method (Przybilla et al. 2006; Firnstein & Przybilla 2006; Schiller & Przybilla 2006), by up to  $\sim 0.2$  dex. One object is found to show super-solar metallicity. The abundance distribution of the heavier elements follows a scaled solar pattern while the light elements have been affected by mixing with CN-cycled matter.

### 4. Results and discussion

The non-LTE computations reduce random errors and remove systematic trends in the analysis. Inappropriate LTE analyses tend to systematically underestimate iron group abundances and overestimate the light and  $\alpha$ -process element abundances by up to factors of 2-3 (most notable for M31-41-3654, while M31-41-3712 is less affected). This is

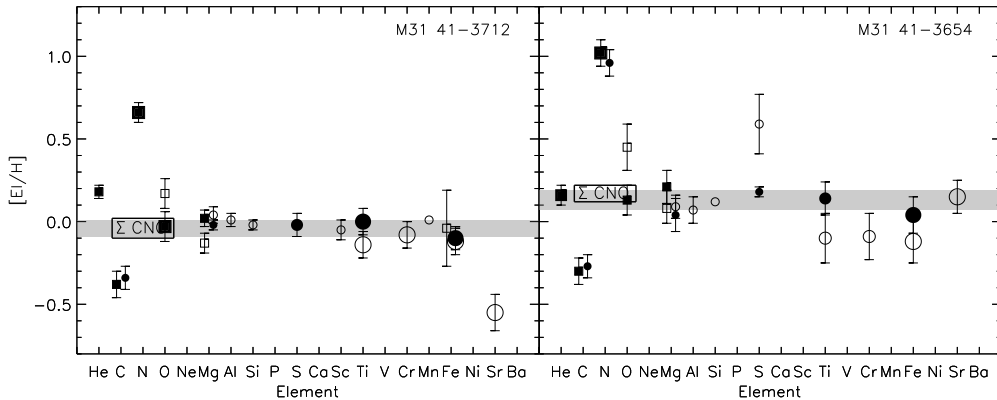


FIGURE 1. Preliminary results from the elemental abundance analysis for our two sample stars, relative to the solar composition (logarithmic scale, Grevesse & Sauval 1998). Filled symbols denote non-LTE, open symbols LTE results. The symbol size codes the number of spectral lines analysed – small: 1 to 5, medium: 6 to 10, large: more than 10. Boxes: neutral, circles: single-ionized species. The error bars represent  $1\sigma$ -uncertainties from the line-to-line scatter. The grey shaded area marks the deduced metallicity of the objects within  $1\sigma$ -errors. The non-LTE abundance analyses imply a scaled solar abundance distribution for the M31 objects. An exception are the light elements which have been affected by mixing with nuclear-processed matter.

because of the different responses of these species to radiative and collisional processes in the microscopic picture, which is explained by fundamental differences of their detailed atomic structure. This is not taken into account in LTE. Contrary to common assumptions, significant non-LTE abundance corrections of  $\sim 0.3$  dex can be found even for the weakest lines ( $W_\lambda \sim 10$  mÅ). Non-LTE abundance uncertainties amount to typically 0.05–0.10 dex (random) and  $\sim 0.10$  dex (systematic  $1\sigma$ -errors). Note that line-blocking effects increase with metallicity, such that photon mean-free paths are reduced in metal-rich environments and the non-LTE effects correspondingly. This is the reason why non-LTE effects in these objects close to the Eddington limit are similar to those in less-extreme Galactic BA-type supergiants with – on average – lower metallicity.

Fundamental stellar parameters and light element abundances allow us to discuss the two M31 objects in the context of stellar evolution. The comparison with evolutionary tracks for rotating massive stars is made in Fig. 2, which also summarises results from a Galactic sample of BA-SGs. The M31 supergiants extend the sample towards higher luminosities/stellar masses than possible in the Galactic study, and towards higher metallicity. Both objects appear to cross the Hertzsprung-Russell diagram towards the red supergiant stage for the first time, because of the absence of extremely high helium abundances and N/C ratios expected for stars entering the Wolf-Rayet phase. The predicted trend of increased chemical mixing (strong N and moderate He enrichment, C depletion and almost constant O as a result of the action of the CNO-cycle and transport to the stellar surface because of meridional circulation and dynamical instabilities) with increasing stellar mass is qualitatively recovered. Note a group of highly processed stars at  $M_0 < 15 M_\odot$ , which suggests an extension of blue loops towards higher temperatures than predicted. The observed N/C ratios are generally higher than indicated by theory. Stellar evolution computations accounting for the interplay of rotation and magnetic fields (e.g. Maeder & Meynet 2005) may resolve this discrepancy as they predict a much higher efficiency for chemical mixing. Also the recent revision of the cross-section for the bottleneck reaction  $^{14}\text{N}(p,\gamma)^{15}\text{O}$  in the CN-branch of the CNO-cycle by almost a factor 2 (Lemut et al. 2006) will be of importance.

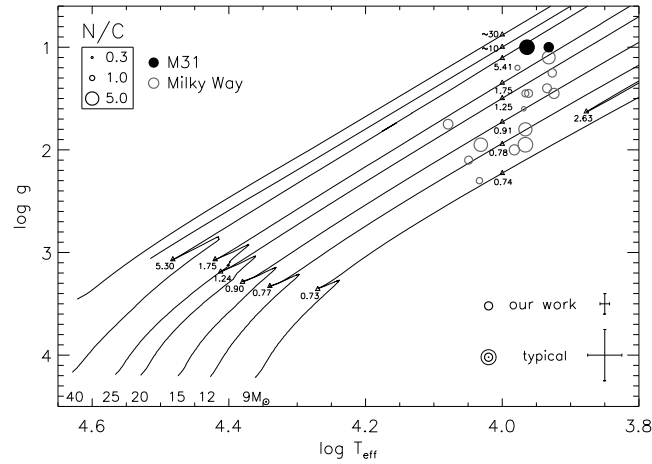


FIGURE 2. Observational constraints on massive star evolution: N/C ratios as tracers of mixing with nuclear-processed material. Displayed are evolution tracks for rotating stars ( $v_{\text{ini}} = 300$  km/s, with marks indicating N/C ratios from the models: Meynet & Maeder 2003) at solar metallicity. The model computations adopt an initial N/C  $\sim 0.3$ . Observed N/C ratios (typical values are indicated in the box) for a sample of Galactic BA-SGs (Przybilla et al. 2006; Firnstein & Przybilla 2006; Schiller & Przybilla 2006) and for the two (slightly) metal-rich M31 objects of the present work are indicated, all analysed in a homogeneous way. Error bars as characteristic for our work and for similar studies from the literature are given.

Finally, improved stellar parameter allow for a re-evaluation of the two M31 supergiants in the empirical calibration of the FGLR (Kudritzki et al. 2003). Two factors play a rôle in this context: a revision of the previously used photometric data of Magnier et al. (1992), which has been shown to suffer from systematic uncertainties (Massey et al. 2006), and the extended wavelength coverage (and high S/N) of the ESI spectra, which allows the atmospheric parameters to be constrained more precisely. As a consequence some of the largest deviations from the empirical relation can be explained.

#### REFERENCES

- Blair, W. P., Kirshner, R. P. & Chevalier, R. A. (1982). *ApJ* **254**, 50-69.  
 Dennefeld, M. & Kunth, D. (1981). *AJ* **86**, 989-997.  
 Firnstein, M. & Przybilla, N. (2006). *Proceedings of Science*, PoS(NIC-IX)095.  
 Grevesse, N. & Sauval, A.J. (1998). *Space Sci. Rev.* **85**, 161-174  
 Kudritzki, R. P., Bresolin, F. & Przybilla, N. (2003). *ApJ* **582**, L83-L86  
 Kurucz, R.L. (1993). Kurucz CD-ROM No. 13 (Cambridge, Mass.: SAO).  
 Lemut, A., Bemerer, D., Confortola, F. et al. (2006). *Physics Letters B* **634**, 483-487.  
 Maeder, A. & Meynet, G. (2005). *A&A* **440**, 1041-1049.  
 Meynet, G. & Maeder, A. (2003). *A&A* **404**, 975-990.  
 Magnier, E. A., Lewin, W. H. G., van Paradijs, J. et al. (1992). *A&AS* **96**, 379-388.  
 Massey, P., Olsen, K. A. G., Hodge, P. W., Strong, S. B. et al. (2006). *AJ* **131**, 2478-2496.  
 Przybilla, N. (2002). Ph.D. Thesis, University Munich.  
 Przybilla, N., Butler, K. & Kudritzki, R.P. (2001). *A&A* **379**, 936-954.  
 Przybilla, N., Butler, K., Becker, S.R. & Kudritzki, R. P. (2006). *A&A* **445**, 1099-1126.  
 Schiller, F. & Przybilla, N. (2006). *Proceedings of Science*, PoS(NIC-IX)174.  
 Smartt, S. J., Crowther, P. A., Dufton, P. L. et al. (2001). *MNRAS* **325**, 257-272.  
 Trundle, C., Dufton, P. L., Lennon, D. J. et al. (2002). *A&A* **395**, 519-533.  
 van den Bergh, S. (1999). *A&AR* **9**, 273-318.  
 Venn, K. A., McCarthy, J. K., Lennon, D. J. et al. (2000). *ApJ* **541**, 610-623.